JOC The Journal of Organic Chemistry

Article

pubs.acs.org/joc

DFT Study of the Mechanism and Origin of Enantioselectivity in Chiral BINOL-Phosphoric Acid Catalyzed Transfer Hydrogenation of Ketimine and α-Imino Ester Using Benzothiazoline

Yukihiro Shibata and Masahiro Yamanaka*

Department of Chemistry and Research Center for Smart Molecules, Faculty of Science, Rikkyo University, 3-34-1 Nishi-Ikebukuro, Toshima-ku, Tokyo 171-8501, Japan

Supporting Information

ABSTRACT: Benzothiazoline is an efficient reducing agent for the chiral BINOL-phosphoric acid catalyzed enantioselective transfer hydrogenation of ketimines and α-imino esters to afford the corresponding amines with high enantioselectivities. DFT studies (M05-2X/6-31G*//ONIOM(B3LYP/6-31G*:HF/3-21G)) revealed the reaction mechanism and the origin of the high enantioselectivity in the present BINOL-phosphoric acid catalyzed transfer hydrogenation of ketimines and α-imino esters using benzothiazoline. The reaction mechanism is similar to that reported in the asymmetric transfer hydrogenation of ketimines using Hantzsch ester. Phosphoric acid simultaneously activates ketimine (α-imino ester) and benzothiazoline to form cyclic transition structures. The high enantioselectivity is attributed to the steric interaction between the substituents at the 3,3′-positions of BINOL-phosphoric acid and substrates. In contrast to the C_2-symmetrical Hantzsch ester, the readily tunable 2-aryl substituent of unsymmetrical benzothiazoline plays a significant role in the steric interaction, influencing the asymmetric induction. This feature is responsible for the advantage of benzothiazoline over Hantzsch ester.

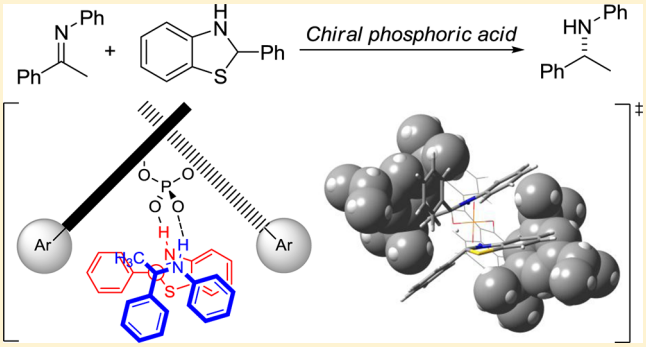

INTRODUCTION

The enantioselective organocatalytic hydrogenation of ketimines[1] and α-imino esters[2] has attracted considerable interest due to its straightforward approach for the preparation of optically pure amines and α-amino acid derivatives. In this reaction, various chiral phosphoric acids[3] have recently emerged as efficient chiral Brønsted acid catalysts that activate ketimines and α-imino esters. Rueping et al.[1a,d,e,h] and List et al.[1b] developed the asymmetric transfer hydrogenation of ketimines using chiral BINOL-phosphoric acid bearing bulky aryl substituents at the 3,3′-positions. The bulky aryl substituents were necessary for the high enantioselectivity in this reaction. By using an analogous chiral phosphoric acid, MacMillan et al.[1c] and List et al.[1f,j] reported the reductive amination of a wide range of ketones. Antilla et al.[2a] and You et al.[2b] independently reported the asymmetric transfer hydrogenation of α-imino esters, which is an attractive route to optically pure α-amino acids. In those reactions, the reducing agent was limited to Hantzsch ester, a widely known synthetic mimic of nicotinamide adenine dinucleotide (NADH). DFT computational studies of the present hydrogenation of ketimines using Hantzsch ester afforded much insight into the reaction mechanism. Goodman et al.[4] and Himo et al.[5] interpreted the reaction mechanism of the chiral BINOL-phosphoric acid catalyzed asymmetric transfer hydrogenation of ketimines using Hantzsch ester. In their elegant computational approach, the reaction mechanism and asymmetric induction were explained by a cyclic transition state (TS): the Brønsted acidic site (proton) electrophilically activated ketimines, whereas the basic site (phosphoryl oxygen) formed a hydrogen bond with Hantzsch ester. On the other hand, Akiyama et al. recently developed benzothiazoline as a novel biomimetic hydrogen source in the phosphoric acid catalyzed enantioselective hydrogenation of ketimines and α-imino esters (Scheme 1).[6] The synthetic utility of benzothiazolines lies in their potential to control both reactivity and stereoselectivity by tuning their electronic and steric properties (e.g., substituent effect of R^3). In a manner similar to Hantzsch ester hydrogenation, the bulky aryl substituents at the 3,3′-positions of BINOL-phosphoric acid were essential for the high enantioselectivity. Therefore, the simultaneous activation of the imino group and benzothiazoline by BINOL-phosphoric acid was predicted and a cyclic TS would promote this reaction. Such a bifunctional activation process via a hydrogen-bonding interaction has emerged as an important paradigm of organocatalysis. We herein theoretically investigated the reaction mechanism and the origin of the high enantioselectivity observed in the chiral BINOL-phosphoric acid catalyzed benzothiazoline hydrogenation of ketimines and α-imino esters.

Received: January 31, 2013
Published: March 25, 2013

dx.doi.org/10.1021/jo4002195 | J. Org. Chem. 2013, 78, 3731−3736

Scheme 1. BINOL-Phosphoric Acid Catalyzed Enantioselective Hydrogenation of Ketimines and α-Imino Esters with Benzothiazolines

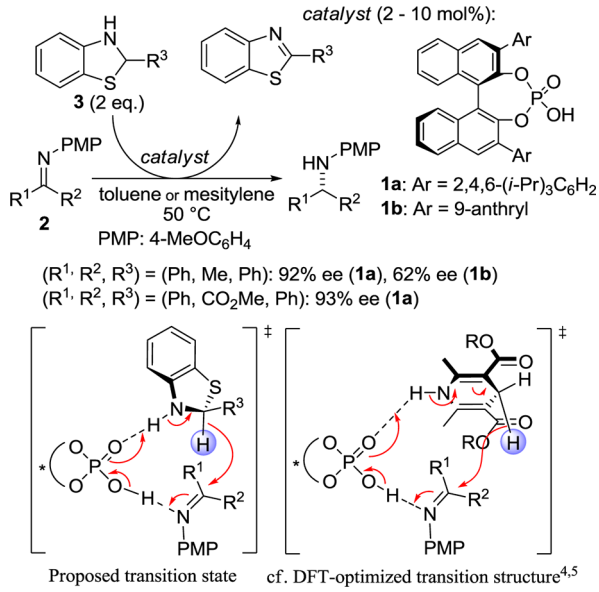

CHEMICAL MODEL AND COMPUTATIONAL METHODS

Previous DFT calculations[4,5] of the Hantzsch ester hydrogenation suggested that the present benzothiazoline hydrogenation should also proceed via a cyclic TS through two hydrogen bonds. The Brønsted acidic site (proton) would activate the imino groups, whereas the Lewis basic site (phosphoryl oxygen) would abstract the proton to induce hydride transfer and aromatization of benzothiazolines. In the simplified chemical model, the benzene rings of BINOL-phosphoric acid and benzothiazoline were removed to reduce computational cost, and biphenol-phosphoric acid (**cat**), ketimine (**El**), and thiazoline (**Nu**) were used. To elucidate the bifunctionality of BINOL-phosphoric acid, two possible pathways (path 1, monocoordination model; path 2, dicoordination model) of the benzothiazoline hydrogenation were first compared using the simplified chemical model (Scheme 2). Focusing on the 3,3′-substituent effect of the phosphoric acid catalyst, 2,4,6-(*i*-Pr)$_3$C$_6$H$_2$- and 9-anthryl-substituted BINOL-phosphoric acids were employed (**1a**, Ar = 2,4,6-(*i*-Pr)$_3$C$_6$H$_2$; **1b**, Ar = 9-anthryl) for the transfer hydrogenation of ketimine (**2a**) with benzothiazoline (**3**). The substituent effect on the α-imino ester (**2b**) was also addressed. A realistic chemical model based on the ideal transition structure of the simplified chemical model was used to investigate steric interaction and asymmetric induction. All calculations were performed with the Gaussian 03 package.[7] Geometries were fully optimized by ONIOM (B3LYP/6-31G*:HF/3-21G)[8] calculations and characterized by frequency calculations. For the realistic chemical models, single-point energy calculations of the ONIOM-optimized structures were evaluated at the M05-2X/6-31G* level.[9,10] According to our previous reports,[11] the 3,3′-substituents (Ar) and the benzene rings of the catalyst and the substrates (and also the ester group in **2b**) were calculated at the lower level layer in the ONIOM calculation to reduce computational cost (blue color in Figure 1). Free energies were also computed for the gas phase. Solution-phase energies were evaluated by single-point energy calculations using M05-2X/6-31G* with the polarizable continuum model (PCM, toluene, ε = 2.379).[12]

RESULTS AND DISCUSSION

Two pathways (path 1, monocoordination model; path 2, dicoordination model) in the simplified chemical model were first explored. Zwitterionic complexes **CPmi**[13] (Scheme 2, path 1) and **CPi** (Scheme 2, path 2) are reversibly formed from **cat**,

Scheme 2. Possible Reaction Mechanisms of the Phosphoric Acid Catalyzed Benzothiazoline Hydrogenation

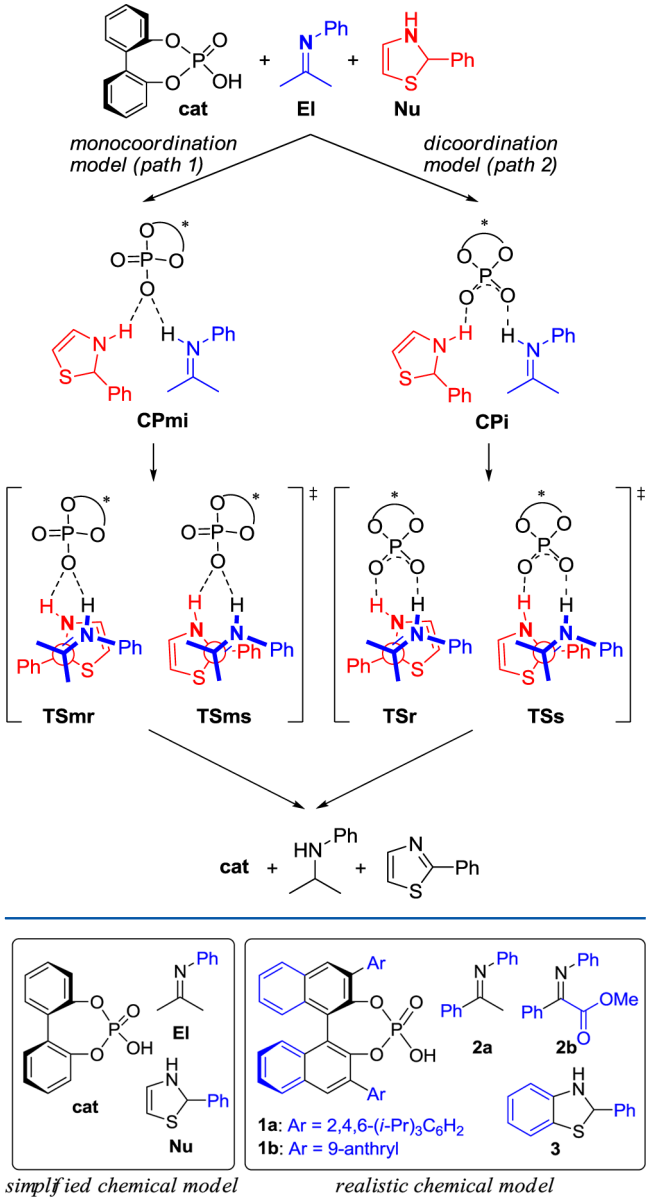

Figure 1. Chemical models.

El, and **Nu** through the protonation of **El** in their neutral hydrogen-bonding complexes. The intramolecular nucleophilic attack of **Nu** (**TS** and **TSm**) yields a product. In both pathways, the two possible diastereomeric TSs (**TSr** and **TSs**) correspond to the absolute configuration of **Nu**. The phenyl group of **Nu** is arranged in a nearly antiperiplanar (**TSr**) or synclinal (**TSs**) fashion with respect to the C═N bond of **El**, respectively.[14] The energy profile has the following features: (1) path 2 is energetically more favored than path 1, and (2) **TSr** is more stable than **TSs** in both reaction pathways (Figure 2). The energetically preferred dicoordination model (path 2) is due to the bifunctional cooperativity of the phosphoric acid moiety, which is found in several phosphoric acid catalyzed asymmetric reactions.[4,5,11,15] Almost the same two P−O bonds (**TSr**, 1.512, 1.508 Å; **TSs**, 1.513, 1.504 Å) are observed in path 2, and hence, the negative charge is delocalized over the O−P−O fragment. In contrast, the two P−O bonds of **TSms** and **TSmr**

dx.doi.org/10.1021/jo4002195 | J. Org. Chem. 2013, 78, 3731−3736

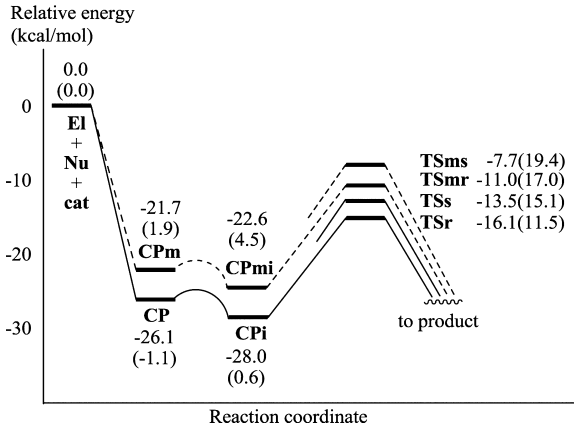

Figure 2. Energy profiles of the monocoordination model (Scheme 2, path 1) and dicoordination model (Scheme 2, path 2). The potential energy of the sum of **cat**, **Nu**, and **El** is set to 0. Free energies are shown in parentheses.

in path 1 are regarded as a P═O double bond (**TSmr**, 1.490 Å; **TSms**, 1.487 Å) and a P−O single bond (**TSmr**, 1.530 Å; **TSms**, 1.531 Å). The dicoordination transition structure is well stabilized by the resonance stabilization of the O−P−O fragment in combination with the hydrogen-bonding interaction between the substrates and the catalyst (Figure 3). The two NH moieties of **TSr** or **TSs** are directed toward **cat** via the hydrogen-bonding network, and hence, the absolute configuration of **Nu** very much affects the NH−O coordination structures in **TS**. Depending on the absolute configuration of **Nu**, one NH moiety is located either close to (**TSr**) or far away from (**TSs**) the other NH moiety. **TSr** provides an effective

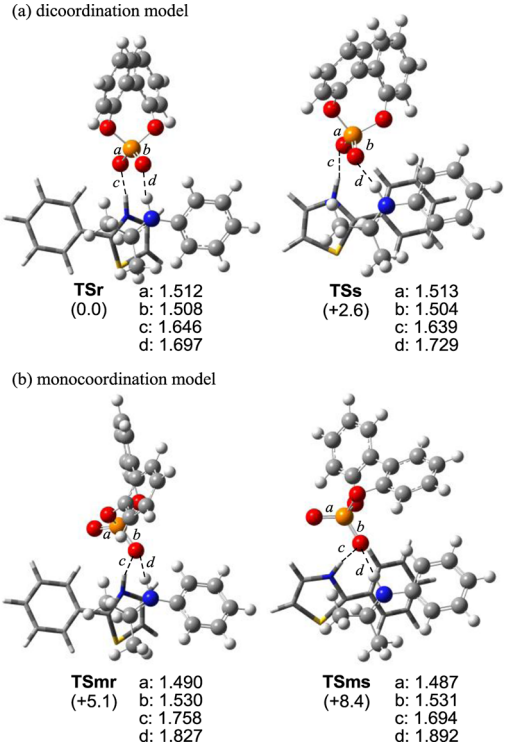

Figure 3. 3D structures of **TSr**, **TSs**, **TSmr**, and **TSms** (C, gray; O, red; N, blue; P, orange; S, yellow; **cat** and **El**, ball and stick model; **Nu**, tube model). Bond lengths are in Å. Relative energies (kcal/mol) are shown in parentheses.

coordination structure for two hydrogen-bonding interactions (1.646, 1.697 Å) and is relatively stable compared to **TSs** (1.639, 1.729 Å).

It was experimentally confirmed that the asymmetric induction in the present reaction was very much affected by the substituents at the 3,3′-positions of BINOL-phosphoric acids. The sterically demanding 2,4,6-(i-Pr)$_3$C$_6$H$_2$ groups at the 3,3′-positions would construct an appropriate asymmetric environment that would yield the highest enantioselectivity for both ketimines and α-imino esters. This indicates that the present benzothiazoline hydrogenation of ketimines and α-imino esters would proceed through a similar transition structure. To elucidate the major factor contributing to the asymmetric induction in the benzothiazoline hydrogenation of ketimines and α-imino esters, possible diastereomeric transition structures leading to the major and minor enantiomers were explored on the basis of the promised dicoordination model (e.g., **TSr** and **TSs**). In the realistic chemical model for the benzothiazoline hydrogenation of **2a** or **2b** catalyzed by **1a** or **1b** (**TS-A**, **1a** and **2a**; **TS-B**, **1b** and **2a**; **TS-C**, **1a** and **2b**), there are eight possible transition structures corresponding to the enantiofacial selection (leading to major and minor enantiomers, **TS**α and **TS**β), two geometric conformations of the imino group (*anti* and *syn* conformations with respect to the two phenyl groups, **TS**$_{anti}$ and **TS**$_{syn}$), and two absolute configurations of benzothiazoline (*S* and *R*, **TSs** and **TSr**) (Scheme 3). In the case of **2a**, the relative energies of the four diastereomeric transition structures leading to the major enantiomer (**TS**α**-A** and **B**, left in Scheme 3) show a matched or mismatched pair between the geometric conformation of **2a** and the absolute configuration of **3**.[16] Whereas *anti* ketimine and (*S*)-benzothiazoline constitute a matched pair (e.g., **TS**α**s**$_{anti}$**-A** and **-B**), *syn* ketimine is matched to (*R*)-benzothiazoline (e.g., **TS**α**r**$_{syn}$**-A** and **B**). The reverse tendency for the matched configurations of ketimine and benzothiazoline was observed in the four diastereomeric transition structures leading to the minor enantiomer (**TS**β**-A** and **-B**, right in Scheme 3). In spite of the thermodynamic stability of *anti* ketimine, the most energetically favored transition structures include *syn* ketimine (**TS**α**r**$_{syn}$**-A,B** and **TS**β**s**$_{syn}$**-A,B**). The sterically compact *syn* ketimine is preferred to *anti* ketimine in combination with the suitably configured benzothiazoline for fitting into the relatively small chiral space of BINOL-phosphoric acid.[17] **TS**β**s**$_{syn}$**-A** is 4.9 kcal/mol higher in energy than **TS**α**r**$_{syn}$**-A**. This is qualitatively consistent with the experimentally observed high enantioselectivity. When the 2,4,6-(i-Pr)$_3$C$_6$H$_2$ group is replaced by the 9-anthryl group, the relative energy difference between **TS**α**r**$_{syn}$**-B** and **TS**β**s**$_{syn}$**-B** decreases dramatically to 1.5 kcal/mol, in good agreement with the experimental results, in which the enantioselectivity is reduced from 92% ee (**1a**) to 62% ee (**1b**). This indicates that the energy difference between **TS**α**r**$_{syn}$ and **TS**β**s**$_{syn}$ affecting the stereoselectivity would be dominated mostly by the steric interaction at the 3,3′-positions of BINOL-phosphoric acid. In the case of **2b**, a similar tendency of the relative stability in **TS**α is observed, and **TS**α**r**$_{syn}$**-C** is the most stable in **TS**α**-C**. On the other hand, the ester group of **2b** affects the relative stability of **TS**β, and **TS**β**s**$_{anti}$**-C** is the most stable in **TS**β**-C**. **TS**α**r**$_{syn}$**-C** is 5.3 kcal/mol lower in energy than **TS**β**s**$_{anti}$**-C**. Almost the same energy difference between the most energetically favored **TS**α and **TS**β observed in both **TS-A** and **TS-C** is in good agreement with the same level of enantioselectivity observed experimentally (**2a**, 92% ee; **2b**, 93% ee). Benzothiazoline

dx.doi.org/10.1021/jo4002195 | J. Org. Chem. 2013, 78, 3731−3736

Scheme 3. Schematic Structures and Relative Energies (kcal/mol) of Eight Possible Transition States[a]

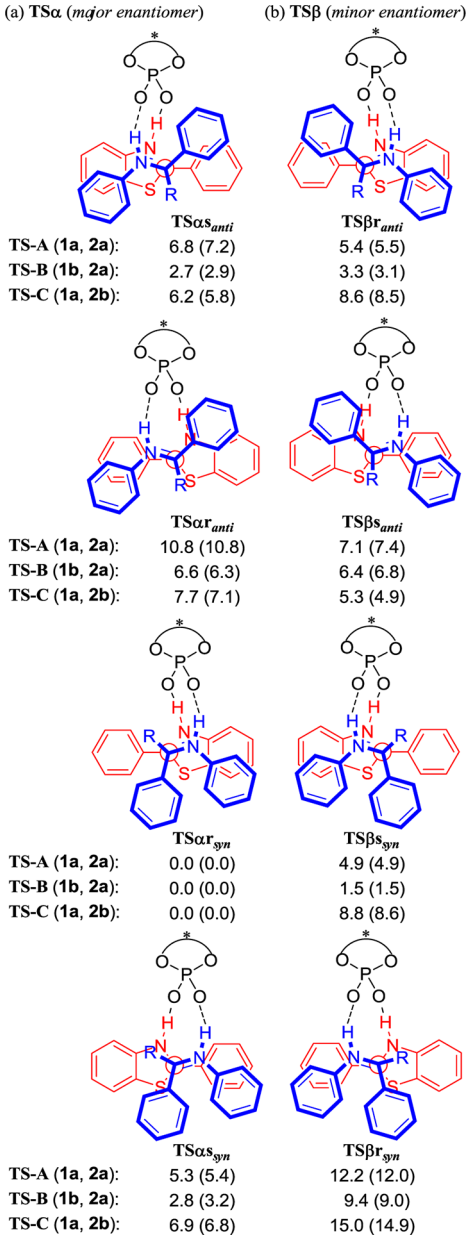

[a]Relative solution phase energies (PCM, toluene) are shown in parentheses.

would be racemized through the ring-opening and -closing reactions under the present experimental conditions. Therefore, (*R*)-benzothiazoline would preferentially react and the reaction would proceed via the most stable **TS*α*r**$_{syn}$.

Structural analysis of the most stable **TS*α*** and **TS*β*** for series **A**−**C** probed the steric interactions that would be regarded as the major factors controlling the stereoselectivity. The phenyl groups of **2a** and **3** are oriented toward the empty pocket of **1a** in **TS*α*r**$_{syn}$**-A** (Figure 4). In contrast, the sterically demanding 2,4,6-(*i*-Pr)$_3$C$_6$H$_2$ group is responsible for the unfavorable steric interactions (purple curve in Figure 4) with the phenyl groups of the substrates in the less stable **TS*β*s**$_{syn}$**-A**. It is noteworthy that the 2-phenyl group of **3** is located close to the 2,4,6-(*i*-Pr)$_3$C$_6$H$_2$ group at the lower right-hand quadrant in **TS*β*s**$_{syn}$**-A** to induce a repulsive interaction. According to the matched

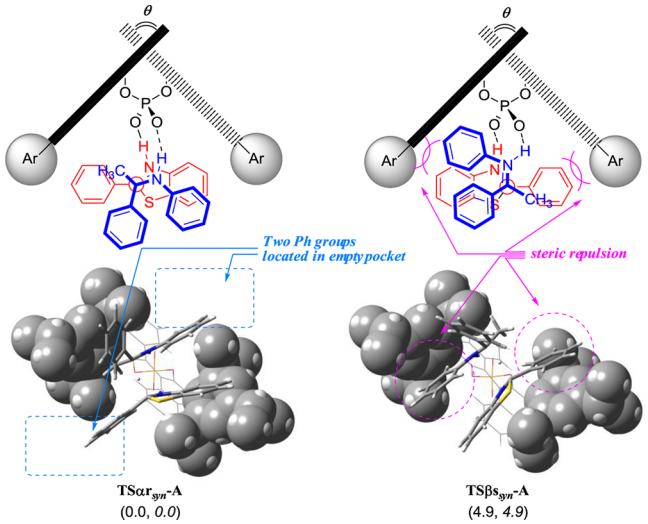

Figure 4. 3D structures and schematic representation models of **TS*α*r**$_{syn}$**-A** and **TS*β*s**$_{syn}$**-A** (3,3′-substituents of BINOL-phosphoric acid, ball model; substrates, tube model). Relative energy differences (kcal/mol) are shown in parentheses. Relative solution-phase energies (PCM, toluene) are shown in italics.

absolute configuration of **3**, the 2-phenyl group of **3** is located in the empty lower left-hand quadrant in **TS*α*r**$_{syn}$**-A** and has no unfavorable steric interaction. Therefore, sterically fine tuning the 2-aryl substituent of benzothiazoline would increase such a repulsive interaction in the less stable diastereomeric **TS** (e.g., **TS*β*s**$_{syn}$) to enhance the enantioselectivity. In fact, benzothiazoline bearing a 2-naphthyl group exhibited higher enantioselectivity (97% ee) than that bearing a 2-phenyl group (92% ee) for **2a**.[6a] This significant substituent effect of benzothiazoline stems from its unsymmetrical structural properties in the transition structure. The repulsive interaction induced by the 2-aryl substituent of benzothiazoline depends on the enantiofacial selectivity of ketimine in each diastereomeric TS (purple curve in Figure 5a). On the other hand, the substituent effect of Hantzsch ester is independent of the enantiofacial selectivity of ketimine. The steric effect of Hantzsch ester in the lower right-hand quadrant should be approximately the same on each diastereomeric TS due to its C_2-symmetric structure (purple curve in Figure 5b). These differences in the steric effects between unsymmetrical benzothiazoline and C_2-symmetric Hantzsch ester result in the major advantage of benzothiazoline.

The steric repulsion between the 9-anthryl group and the phenyl groups of the substrates is also found in **TS*β*s**$_{syn}$**-B**, but its destabilizing effect is relatively small (Figure S2 in the Supporting Information). The insufficient chiral space of **1b** for the asymmetric induction in the present reaction induces unfavorable steric interactions with the substrates, even in the most stable **TS*α*r**$_{syn}$**-B**. Such unfavorable steric interactions deform the catalyst structure, which would be more flexible than the substrate structure. The dihedral angle around the chiral axis of the BINOL unit is larger in **TS*α*r**$_{syn}$**-B** (θ = 58.3°) than in **TS*α*r**$_{syn}$**-A** (θ = 53.5°). It remains unchanged in **TS*β*s**$_{syn}$**-B** (θ = 58.9°) and becomes larger in **TS*β*s**$_{syn}$**-A** (θ = 56.6°). The deformation of the catalyst structure destabilizes **TS*α*r**$_{syn}$**-B** to decrease the relative energy differences of the diastereomeric transition structures. In a manner similar to that for **TS*α*r**$_{syn}$**-A**, the phenyl groups of **2b** and **3** are also oriented toward the empty pocket of **1a** in **TS*α*r**$_{syn}$**-C**. On the other

dx.doi.org/10.1021/jo4002195 | J. Org. Chem. 2013, 78, 3731−3736

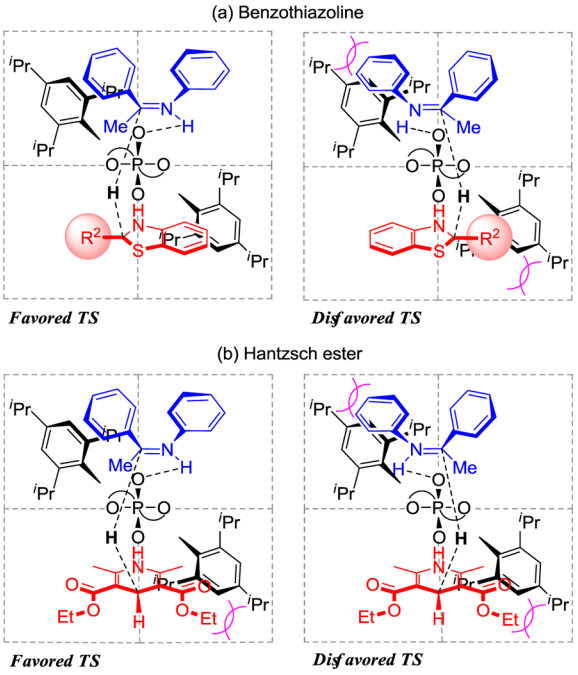

Figure 5. Schematic representations of steric interactions in the diastereomeric transition structures for two reducing agents: (a) benzothiazoline; (b) Hantzsch ester.

hand, **TSβs$_{syn}$-C** is less stable than **TSβs$_{anti}$-C** because of the repulsive interaction between the ester group of **2b** and the phenyl group of **3**. As a result, **TSβs$_{anti}$-C** becomes the most stable TS in **TSβ**, leading to the minor enantiomer (Figure 6 and Figure S3 (Supporting Information)).

CONCLUSION

DFT studies of the chiral BINOL-phosphoric acid catalyzed asymmetric transfer hydrogenation of ketimine and α-imino ester with benzothiazoline were carried out to reveal the reaction mechanism as well as the origin of the high enantioselectivity. The reaction mechanism is similar to that reported in the transfer hydrogenation of ketimines with Hantzsch ester, in which the bifunctionality of the phosphoric acid plays a significant role in the simultaneous activation of ketimines and Hantzsch ester. In the present BINOL-phosphoric acid catalyzed benzothiazoline hydrogenation, the Brønsted acidic site (proton) electrophilically activates ketimines, whereas the basic site (phosphoryl oxygen) coordinates benzothiazoline to accelerate hydride transfer. It is noteworthy that *syn* ketimine is preferred to *anti* ketimine in TS because of the compact chiral space constructed by the substituents at the 3,3′-positions of BINOL-phosphoric acid. The matched or mismatched pair between the geometric conformation of the imino group and the absolute configuration of benzothiazoline depends on the enantiofacial selection. High enantioselectivity is achieved by the steric interaction with the 3,3′-substituents of BINOL-phosphoric acid. In contrast to C_2-symmetrical Hantzsch ester, unsymmetrical benzothiazoline induces a matched or mismatched pair of substrate orientations in TS. The present TS model readily explained the major advantage of sterically and electronically tunable benzothiazoline. The repulsive interaction between the 2-aryl substituent of benzothiazoline and the 3,3′-substituents of BINOL-phosphoric acid exists only in the energetically disfavored TS leading to the minor enantiomer. This indicates that modification of the 2-aryl substituent of benzothiazoline would affect the stereochemical outcome of the product.

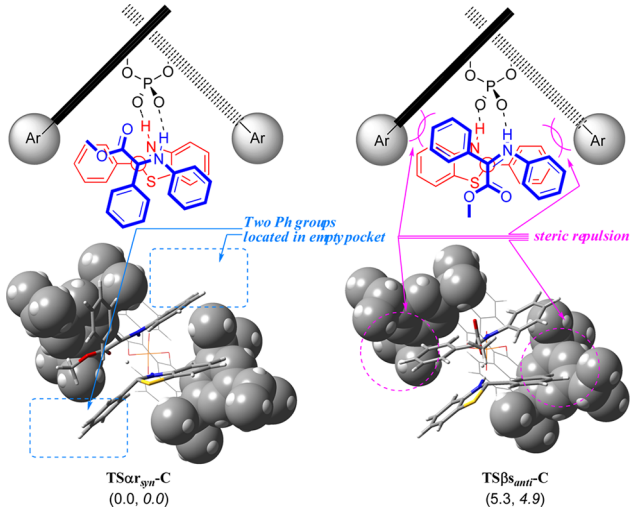

Figure 6. 3D structures and schematic representation models of **TSαr$_{syn}$-C** and **TSβs$_{anti}$-C** (3,3′-substituents of BINOL-phosphoric acid, ball model; substrates, tube model). Relative energy differences (kcal/mol) are shown in parentheses. Relative solution-phase energies (PCM, toluene) are shown in italics.

ASSOCIATED CONTENT

Supporting Information

Figures and tables giving computational details (Cartesian coordinates and absolute energies for stationary points) and text giving the complete ref 7. This material is available free of charge via the Internet at http://pubs.acs.org.

AUTHOR INFORMATION

Corresponding Author

*E-mail for M.Y.: myamanaka@rikkyo.ac.jp.

Notes

The authors declare no competing financial interest.

ACKNOWLEDGMENTS

We thank Prof. T. Akiyama for helpful discussions. This work was supported by a Grant-in-Aid for Scientific Research on Innovative Areas “Advanced Molecular Transformations by Organocatalysts” from The Ministry of Education, Culture, Sports, Science and Technology of Japan.

REFERENCES

(1) For the organocatalytic transfer hydrogenation of ketimines using Hantzsch ester, see: (a) Rueping, M.; Sugiono, E.; Azap, C.; Theissmann, T.; Bolte, M. *Org. Lett.* **2005**, *7*, 3781−3783. (b) Hoffmann, S.; Seayad, A.; List, B. *Angew. Chem., Int. Ed.* **2005**, *44*, 7424−7427. (c) Storer, R. I.; Carrere, D. E.; Ni, Y.; MacMillan, D. W. C. *J. Am. Chem. Soc.* **2006**, *128*, 84−86. (d) Rueping, M.; Antonchick, A. P.; Theissmann, T. *Angew. Chem., Int. Ed.* **2006**, *45*, 3683−3686. (e) Rueping, M.; Antonchick, A. P.; Theissmann, T. *Angew. Chem., Int. Ed.* **2006**, *45*, 6751−6755. (f) Zhou, J.; List, B. *J. Am. Chem. Soc.* **2007**, *129*, 7498−7499. (g) Guo, Q.-S.; Du, D.-M.; Xu, J. *Angew. Chem., Int. Ed.* **2008**, *47*, 759−762. (h) Rueping, M.; Antonchick, A. P. *Angew. Chem., Int. Ed.* **2008**, *47*, 5836−5838. (i) Li, G.; Antilla, J. C. *Org. Lett.* **2009**, *11*, 1075−1078. (j) Wakchaure, V. N.; Zhou, J. A.; Hoffmann, S.; List, B. *Angew. Chem., Int. Ed.* **2010**, *49*, 4612−4614.

(2) For the organocatalytic transfer hydrogenation of α-imino esters using Hantzsch ester, see: (a) Li, G. L.; Liang, Y. X.; Antilla, J. C. *J. Am. Chem. Soc.* **2007**, *129*, 5830−5831. (b) Kang, Q.; Zhao, Z. A.; You, S. L. *Adv. Synth. Catal.* **2007**, *349*, 1657−1660; Corrigendum: *Adv. Synth. Catal.* **2007**, *349*, 2075. (c) Kang, Q.; Zhao, Z. A.; You, S. L. *Org. Lett.* **2008**, *10*, 2031−2034.
(3) For selected reviews, see: (a) Akiyama, T.; Itoh, J.; Fuchibe, K. *Adv. Synth. Catal.* **2006**, *348*, 999−1010. (b) Akiyama, T. *Chem. Rev.* **2007**, *107*, 5744−5758. (c) Terada, M. *Synthesis* **2010**, 1929−1982. (d) Rueping, M.; Kuenkel, A.; Atodiresei, I. *Chem. Soc. Rev.* **2011**, *40*, 4539−4549. (e) Yu, J.; Shi, F.; Gong, L.-Z. *Acc. Chem. Res.* **2011**, *44*, 1156−1171.
(4) Simón, L.; Goodman, J. M. *J. Am. Chem. Soc.* **2008**, *130*, 8741−8747.
(5) Marcelli, T.; Hammar, P.; Himo, F. *Adv. Synth. Catal.* **2009**, *351*, 525−529.
(6) (a) Zhu, C.; Akiyama, T. *Org. Lett.* **2009**, *11*, 4180−4183. (b) Zhu, C.; Akiyama, T. *Adv. Synth. Catal.* **2010**, *352*, 1846−1850. (c) Henseler, A.; Kato, M.; Mori, K.; Akiyama, T. *Angew. Chem., Int. Ed.* **2011**, *50*, 8180−8183. (d) Saito, K.; Akiyama, T. *Chem. Commun.* **2012**, *48*, 4573−4575. (e) Sakamoto, T.; Mori, K.; Akiyama, T. *Org. Lett.* **2012**, *14*, 3312−3315.
(7) Frisch, M. J., et al. *Gaussian 03, Revision E.01*; Gaussian, Inc., Wallingford, CT, 2004.
(8) For selected examples, see: (a) Dapprich, S.; Komaromi, I.; Byun, K. S.; Morokuma, K.; Frisch, M. J. *J. Mol. Struct. (THEOCHEM)* **1999**, *461−462*, 1−21. (b) Svensson, M.; Humbel, S.; Morokuma, K. *J. Chem. Phys.* **1996**, *105*, 3654−3661. (c) Vreven, T.; Morokuma, K. *J. Comput. Chem.* **2000**, *21*, 1419−1432.
(9) Zhao, Y.; Schultz, N. E.; Truhlar, D. G. *J. Chem. Theory Comput.* **2006**, *2*, 364−382.
(10) M05-2X is a good level of theory for studying organocatalysis. See: Simòn, L.; Goodman, J. M. *Org. Biomol. Chem.* **2011**, *9*, 689−700.
(11) (a) Yamanaka, M.; Itoh, J.; Fuchibe, K.; Akiyama, T. *J. Am. Chem. Soc.* **2007**, *129*, 6756−6764. (b) Yamanaka, M.; Hirata, T. *J. Org. Chem.* **2009**, *74*, 3266−3271. (c) Akiyama, T.; Morita, H.; Bachu, P.; Mori, K.; Yamanaka, M.; Hirata, T. *Tetrahedron* **2009**, *65*, 4950−4956. (d) Hirata, T.; Yamanaka, M. *Chem. Asian J.* **2011**, *6*, 510−516.
(12) (a) Cammi, R.; Mennucci, B.; Tomasi, J. *J. Phys. Chem. A* **2000**, *104*, 5631−5637. (b) Cammi, R.; Mennucci, B.; Tomasi, J. *J. Phys. Chem. A* **1999**, *103*, 9100−9108. (c) Cossi, M.; Rega, N.; Scalmani, M.; Barone, V. *J. Chem. Phys.* **2001**, *114*, 5691−5701.
(13) The proton transfer process would exhibit a very flat energy profile that could be ignored in this study; see ref 11a.
(14) In both reaction pathways, two types of diastereomeric complexes directing toward **TSr** and **TSs** should exist with respect to the absolute configuration of **Nu**. Intermediate complexes leading to unfavorable **TSs** were ignored, as those complexes are reversible and are located on the very flat potential energy surface. Therefore, only the intermediate complex leading to favorable **TSr** is described by **CPi** (**CP**).
(15) (a) Simón, L.; Goodman, J. M. *J. Am. Chem. Soc.* **2008**, *130*, 8741−8747. (b) Chen, X.-H.; Wei, Q.; Luo, S.-W.; Xiao, H.; Gong, L.-Z. *J. Am. Chem. Soc.* **2009**, *131*, 13819−13825. (c) Shi, F.-Q.; Song, B.-A. *Org. Biomol. Chem.* **2009**, *7*, 1292−1298. (d) Nan, Li, N.; Chen, X.-H.; Song, J.; Luo, S.-W; Fan, W.; Gong, L.-Z. *J. Am. Chem. Soc.* **2009**, *131*, 15301−15310. (e) Simón, L.; Goodman, J. M. *J. Org. Chem.* **2010**, *75*, 589−597. (f) Zheng, C.; Sheng, Y.-F.; Li, Y.-X.; You, S.-L. *Tetrahedron* **2010**, *66*, 2875−2880. (g) Xu, S.; Wang, Z.; Li, Y.; Zhang, X.; Wang, H.; Ding, K. *Chem. Eur. J.* **2010**, *16*, 3021−3035. (h) Cai, Q.; Zheng, C.; You, S.-L. *Angew. Chem., Int. Ed.* **2010**, *49*, 8666−8669. (i) He, L.; Chen, X.-H.; Wang, D.-N.; Luo, S.-W.; Zhang, W.-Q.; Yu, J.; Ren, L.; Gong, L.-Z. *J. Am. Chem. Soc.* **2011**, *133*, 13504−13518. (j) Simón, L.; Goodman, J. M. *J. Org. Chem.* **2011**, *76*, 1775−1788. (k) Shi, F.; Luo, S.-W.; Tao, Z.-L.; He, L.; Yu, J.; Tu, S.-J.; Gong, L.-Z. *Org. Lett.* **2011**, *13*, 4680−4683. (l) Grayson, M. N.; Pellegrinet, S. C.; Goodman, J. M. *J. Am. Chem. Soc.* **2012**, *134*, 2716−2722. (m) Shi, F.; Xing, G.-J.; Tao, Z.-L.; Luo, S.-W.; Tu, S.-J.; Gong, L.-Z. *J. Org. Chem.* **2012**, *77*, 6970−6979. (n) Wang, H.; Jain, P.; Jon C. Antilla, J. C.; Houk, K. N. *J. Org. Chem.* **2013**, *78*, 1208−1215.
(16) The present benzothiazoline hydrogenation would be the first example of a type II, *Z*-TS on the basis of the Goodman diagram; see ref 4.
(17) These results are related to a similar trend of *syn* ketimine preference in Hantzsch ester reduction; see ref 4.